HEPATOLOGY
Official Journal of the American Association for the Study of Liver Diseases

Deficiency of Carboxylesterase 1/Esterase-x Results in Obesity, Hepatic Steatosis, and Hyperlipidemia

Ariel D. Quiroga,[1,2] Lena Li,[1,2] Martin Trötzmüller,[3] Randy Nelson,[1,2] Spencer D. Proctor,[2,4] Harald Köfeler,[3] and Richard Lehner[1,2,5]

Increased lipogenesis, together with hyperlipidemia and increased fat deposition, contribute to obesity and associated metabolic disorders including nonalcoholic fatty liver disease. Here we show that carboxylesterase 1/esterase-x (Ces1/Es-x) plays a regulatory role in hepatic fat metabolism in the mouse. We demonstrate that Ces1/Es-x knockout mice present with increased hepatic lipogenesis and with oversecretion of apolipoprotein B (apoB)-containing lipoproteins (hepatic very-low density lipoproteins), which leads to hyperlipidemia and increased fat deposition in peripheral tissues. Consequently, Ces1/Es-x knockout mice develop obesity, fatty liver, hyperinsulinemia, and insulin insensitivity on chow diet without change in food intake and present with decreased energy expenditure. Ces1/Es-x deficiency prevents the release of polyunsaturated fatty acids from triacylglycerol stores, leading to an up-regulation of sterol regulatory element binding protein 1c-mediated lipogenesis, which can be reversed with dietary ω-3 fatty acids. *Conclusion:* These studies support a role for Ces1/Es-x in the partitioning of regulatory fatty acids and concomitant control of hepatic lipid biosynthesis, secretion, and deposition. (HEPATOLOGY 2012;56:2188-2198)

The liver is the central metabolic organ that regulates key pathways in lipid metabolism including fatty acid (FA) β-oxidation, lipogenesis, as well as lipoprotein uptake and secretion in response to nutritional and hormonal signals.[1] Dysregulation of hepatic lipid metabolic pathways results in the development of hepatic steatosis, which in turn contributes to the development of chronic hepatic inflammation, insulin resistance, and liver damage.[2,3] We have previously demonstrated that carboxylesterase 3/triacylglycerol hydrolase (Ces3/TGH) (recently annotated Ces1d)[4] plays an important role in the provision of lipid substrates for the assembly of apolipoprotein B (apoB)-containing lipoproteins.[5] Ablation of *Ces3/Tgh/Ces1d* expression in mice leads to decreased plasma lipids, including triacylglycerol (TG) and nonesterified fatty acids (NEFA), along with decreased apoB100 secretion.[6]

Mouse Ces1/Es-x (recently annotated Ces1g)[4] shares ~76% protein sequence identity with mouse Ces3/TGH/Ces1d, including conserved lipase/esterase catalytic triad amino acid residues and regions of the lid domain.[7,8] Hepatic *Ces1/Es-x* expression was found to be augmented in mice fed either a ketogenic[9] or a cholate supplemented[8] diet and is reduced in stearoyl-CoA desaturase-1 (SCD-1)-deficient mice fed a very-low-fat diet.[10] It has also been reported that ectopic expression of *Ces1/Es-x* in McArdle-RH7777 attenuates

Abbreviations: ALT, alanine aminotransferase; apo, apolipoprotein; AST, aspartate aminotransferase; AUC, area under the curve; BAT brown adipose tissue; BSA, bovine serum albumin; CE, cholesteryl ester; Ces, carboxylesterase; CNX calnexin; CYC, cyclophilin; DGAT, diacylglycerol acyltransferase; DHA, docosahexaenoic acid; DIO, diet-induced obesity; DMEM, Dulbecco's Modified Eagle Medium; EPA, eicosapentaenoic acid; Es-x, esterase-x; FAS, fatty acid synthase; FC, free cholesterol; Ldlr, low-density lipoprotein receptor; LpL, lipoprotein lipase; LXR, liver X receptor; MGAT, monoacylglycerol acyltransferase; MTP, microsomal triglyceride transfer protein; NEFA, nonesterified fatty acid; OA, oleic acid; P-407, poloxamer-407; PCR, polymerase chain reaction; PL, phospholipids; PUFA, polyunsaturated fatty acids; RQ, respiratory quotient; SCD, stearoyl-CoA desaturase; SREBP, sterol regulatory element binding protein; TG, triacylglycerol; TGH, triacylglycerol hydrolase; TLC, thin-layer chromatography; UCP-1, uncoupling protein-1; VLDL, very low-density lipoprotein, WAT, white adipose tissue.

From the [1]Department of Pediatrics, University of Alberta, Edmonton, Canada; [2]Group on Molecular and Cell Biology of Lipids, University of Alberta, Edmonton, Canada; [3]Center for Medical Research, Medical University Graz, Graz, Austria; [4]Metabolic and Cardiovascular Diseases Laboratory, University of Alberta, Edmonton, Canada; [5]Department of Cell Biology, University of Alberta, Edmonton, Canada.

Received April 28, 2012; accepted June 8, 2012.

Supported with funds from the Canadian Institutes of Health Research (to R.L.) and by the LipidomicNet project, Grant No. 202272 from the 7th Framework Programme of the European Union (to H.K.). Part of this work was supported by the Canadian Lipoprotein Conference/Merck Research Award to A.D.Q. R.L. is an Alberta Innovates-Health Solutions Scientist. A.D.Q. is a recipient of a postdoctoral fellowship from the Heart and Stroke Foundation of Canada. S.D.P is a Heart and Stroke Foundation of Canada New Investigator.

cellular TG accretion and increases fatty acid oxidation.[11] Here we report that ablation of *Ces1/Es-x* expression in mice results in obesity, fatty liver, and hyperlipidemia by up-regulation of *de novo* lipogenesis and lipoprotein oversecretion. We conclude that Ces1/Es-x is a new player in energy metabolism.

Materials and Methods

Animals. Unless otherwise specified, 5 to 6-month-old female mice were fed *ad libitum* a chow diet. A detailed description of the production of *Ces1/Es-x*$^{-/-}$ mice is presented in the Supporting Information.

Plasma and Tissue Parameters. Plasma and tissue levels of TG, phospholipids (PL), free cholesterol (FC), and cholesteryl esters (CE) were determined by gas chromatography (GC) as described.[6] In some cases TG and PL concentrations were determined by commercial kits. Blood glucose was monitored using blood glucose strips and the Accu-Check glucometer (Roche Diagnostics, Vienna, Austria). Plasma insulin concentration was measured by enzyme-linked immunosorbent assay (ELISA) (Millipore, Bedford, MA). Plasma FA levels were determined using the NEFA C commercial kit according to the manufacturer's protocol (Wako, Japan). Hepatic enzymes were measured using a commercial kit (Biotron Diagnostic, Hemet, CA). Ketone bodies were measured according to manufacturer's instructions (Wako, Japan). For the analyses of plasma and tissue metabolic parameters 6 mice per group were used.

***Analysis of Very-Low Density Lipoprotein (VLDL) Secretion* In Vivo.** After a 12-hour fasting period, mice received an intraperitoneal injection of 1 g/kg body weight of poloxamer-407 (P-407, BASF, Florham Park, NJ). Blood was collected from tail veins before and at different timepoints after the administration of the detergent. Plasma was prepared and TG levels were analyzed by GC. Plasma proteins from these samples were analyzed by immunoblotting. For analysis of newly synthesized apoB, mice were fasted for 4 hours and injected with 100 μL of phosphate-buffered saline (PBS) containing 250 μCi of [^{35}S]methionine by way of tail vein, together with an intraperitoneal injection of P-407. Two hours following P-407 injection, blood samples were collected and plasma was prepared and processed for apoB analyses.[6]

Glucose and Insulin Tolerance Tests and* In Vivo *Insulin Signaling. Prior to glucose tolerance test, mice were fasted overnight. Then a glucose solution (2 g/kg body weight) was administered by oral gavage. Glucose concentration was monitored before and at 15, 30, 60, and 120 minutes postgavage using blood glucose strips. For insulin sensitivity studies, mice were fasted for 6 hours and injected intraperitoneally 1 U bovine insulin/kg body weight. Blood was collected before injection and 15, 30, 60, 120 minutes after injection and glucose levels were determined as described above. For *in vivo* insulin signaling mice were fasted for 12 hours before 0.5 U/kg body weight of bovine insulin or PBS was injected by way of the portal vein. Livers were harvested 5 minutes after injection. Similarly, skeletal muscle and adipose tissue insulin sensitivity was evaluated by injecting 1 U/kg body weight of bovine insulin or PBS intraperitoneally. Skeletal muscles and adipose tissues were harvested 10 minutes after injections. Cell lysates were prepared and western blot analysis was carried out using the following primary antibodies: anti-AKT and anti-p-AKT (Cell Signaling Technology, Beverly, MA). The ratio between p-AKT and AKT was employed to evaluate hepatic insulin sensitivity.

Physical Activity, Oxygen Consumption, and Respiratory Exchange Ratio. Oxygen consumption (VO_2), CO_2 production (VCO_2), and heat production were obtained by indirect calorimetry using the Comprehensive Laboratory Animal Monitoring System (Metabolic cage; Oxymax/CLAMS; Columbus Instruments, Columbus, OH). Physical activity was monitored by dual-axis detection (X, Z) using infrared photocell technology. Total physical activity was calculated by adding Z counts (rearing) to total counts associated with ambulatory movement and typical behavior.

Body Composition Measurements. Body composition was determined in 24-week-old mice using a Minispec whole-body composition analyzer (Bruker Minispec LF90 II, Hamilton, Ontario, Canada).

RNA Isolation and Polymerase Chain Reaction (PCR) Analysis. First-strand complementary DNA (cDNA) synthesis from 2 μg of total RNA was performed using

Address reprint requests to: Richard Lehner, Ph.D., Departments of Pediatrics and Cell Biology and Group on Molecular and Cell Biology of Lipids, University of Alberta, 328 Heritage Medical Research Centre, Edmonton, Alberta, Canada T6G 2S2. E-mail: richard.lehner@ualberta.ca; fax: 780-492-3383.

View this article online at wileyonlinelibrary.com.

DOI 10.1002/hep.25961

Potential conflict of interest: Nothing to report.

Additional Supporting Information may be found in the online version of this article.

Table 1. Plasma and Liver Biochemical Parameters 5-Month-Old Female Mice

	Wildtype	*Ces1/Es-x*$^{-/-}$
Body weight (g)	25.60 ± 1.47	42.37 ± 2.13**
Plasma TG (mg/dL)	46.27 ± 2.38	92.69 ± 4.05**
Plasma FC (mg/dL)	45.34 ± 0.86	92.61 ± 3.59**
Plasma CE (mg/dL)	44.95 ± 6.82	84.85 ± 6.45**
Plasma PL (mg/dL)	71.86 ± 1.67	83.73 ± 9.85*
Liver TG (μg/mg protein)	279.0 ± 20.26	835.7 ± 65.66***
Liver FC (μg/mg protein)	16.44 ± 0.86	23.89 ± 1.60*
Liver CE (μg/mg protein)	9.20 ± 0.85	24.35 ± 1.47**
NEFA (mEq/L)	0.8640 ± 0.068	1.226 ± 0.124*
AST (U/L)	80.20 ± 2.78	99.40 ± 1.36**
ALT (U/L)	38.80 ± 1.15	57.40 ± 2.42**
Glucose (mmol/L)	4.57 ± 0.13	3.88 ± 0.17*
Insulin (ng/mL)	0.36 ± 0.09	0.72 ± 0.07*

n=6.
*$P < 0.05$.
**$P < 0.005$.
***$P < 0.0001$.

Super-Script II reverse transcriptase (Invitrogen) primed by oligo(dT)12-18 primers. The transcripts of Ces1/Es-x were evaluated by PCR analysis. Real-time quantitative (q)PCR was employed to detect other transcripts related to fatty acid oxidation, lipogenesis, and lipolysis. Detailed procedures for real-time qPCR are presented in the Supporting Information. All primers were synthesized at the DNA Core Facility of the University of Alberta. Primers for the various genes are listed in Supporting Table 1.

Labeling Studies. Before the labeling studies, primary mouse hepatocytes were incubated overnight with serum-free Dulbecco's modified Eagle's medium (DMEM). For incorporation of exogenous FA studies (general cellular acyltransferase activity), hepatocytes were incubated in 2 mL of DMEM containing 5 μCi [^{3}H]oleic acid (OA) dissolved in 0.4 mM OA / 0.5% FA-free bovine serum albumin (BSA). After 15, 30, 60, 120, 240, and 480 minutes incubation, cells and media were collected for analysis. Lipids were extracted in chloroform:methanol (2:1, v/v) containing TG, CE, and PL as internal standards. Then lipids were separated by thin-layer chromatography (TLC) on silica gel H TLC plates with the solvent system hexane:isopropyl ether:acetic acid (15:10:1, v/v/v). Lipids were visualized by exposure to iodine, and lipids were recovered and radioactivity determined by scintillation counting. To assess the hepatic lipid biosynthetic capacity, primary hepatocytes were incubated in 2 mL of DMEM containing 10 μCi [^{3}H]acetic acid dissolved in 250 μM nonradiolabeled acetic acid. After a 4-hour incubation, cells and media were collected for analysis. Lipids were extracted, resolved by TLC, and analyzed as described above.

To evaluate the lipid mass secreted by primary hepatocytes, media were collected at 4 hours after incubation with the radiolabeled precursors, lipid extracted, and dissolved in ethanol. TG levels were analyzed by GC. To assess the effect of polyunsaturated fatty acids (PUFA) on lipogenesis, primary mouse hepatocytes were incubated in 2 mL of DMEM with or without 0.25 mM eicosapenatenoic acid (EPA) and 0.25 mM docosahexaenoic acid (DHA) complexed with 0.5% FA-free BSA containing 10 μCi [^{3}H]acetic acid dissolved in 250 μM nonradiolabeled acetic acid. After a 4-hour incubation, cells and media were collected for analysis. Lipids were extracted, resolved by TLC, and analyzed as described above.

SREBP-1c Immunoblotting. Nuclear extracts for sterol regulatory element binding protein 1c (SREBP-1c) studies were prepared as described,[12] and described in the Supporting Information. SREBP-1c immunoblotting was performed with polyclonal anti SREBP-1c antibodies #297 kindly provided by Drs. Michael Brown and Joseph Goldstein (UT Southwestern, Dallas, TX).

Fish Oil Supplementation Studies. Eight-week-old female mice (n = 5/group) were gavaged with 200 μL fish oil (Webber Naturals, Canada) for 4 months. Body weight was monitored every week. At the end of the treatment, animals were sacrificed by cardiac puncture and tissues (including plasma) were flash-frozen in liquid nitrogen or processed for histology.

Additional experimental procedures are described in the Supporting Information.

Statistical Analysis. Data are presented as means ± standard error of the mean (SEM). Statistical significance was evaluated by unpaired two-tailed Student's test. Time course studies were evaluated by two-way analysis of variance (ANOVA) followed by Bonferroni posttest (GraphPad PRISM 4 software). $P < 0.05$ was interpreted as a significant difference.

Results

Experiments were performed in both male and female mice. Both sexes showed a similar phenotype. However, hepatic and plasma lipid levels were slightly higher in females compared to males. Data for female mice are presented herein.

Ces1/Es-x Expression Is Nutritionally Regulated and Is Decreased in Animal Models of Obesity, Fatty Liver, and Insulin Resistance. Hepatic Ces1/Es-x protein levels are very low after a 24-hour fasting period and are increased upon refeeding for 6 hours after a 24-hour fast (Fig. 1A). Hepatic *Ces1/Es-x* expression is

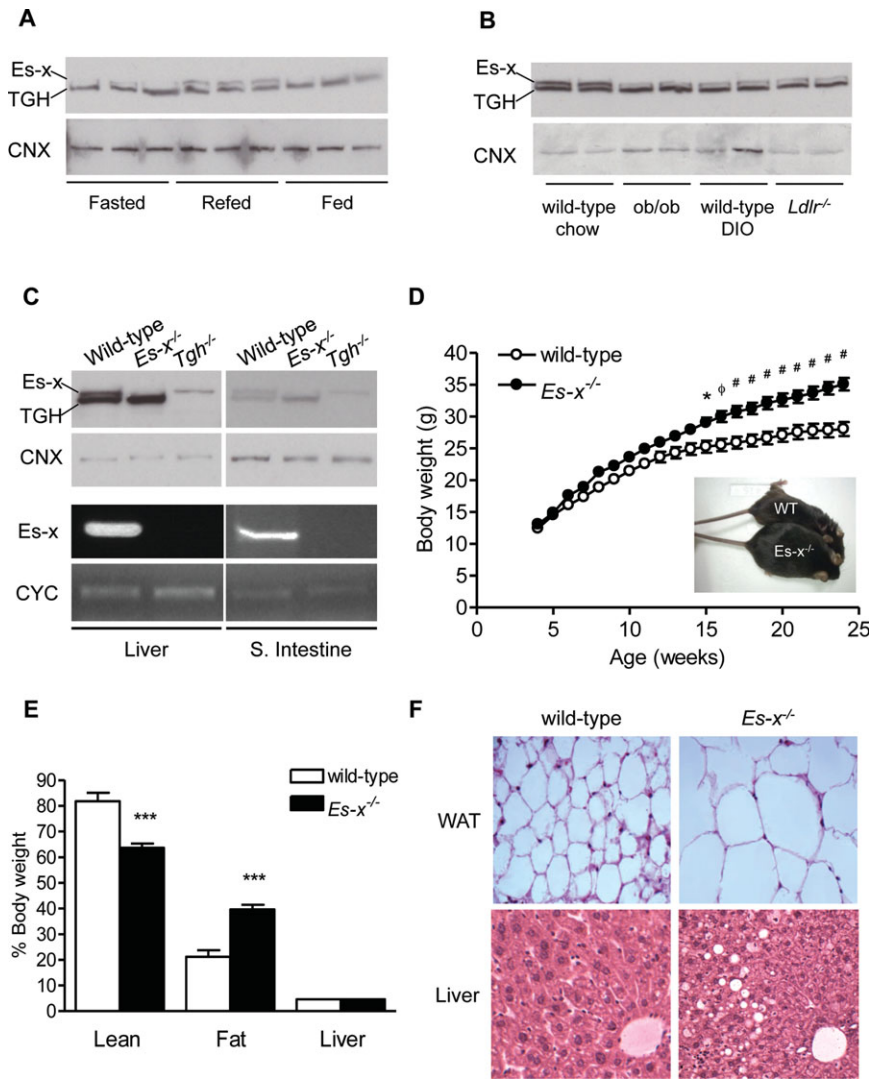

Fig. 1. Ces1/Es-x deficiency results in obesity and hepatic steatosis. (A) Hepatic Ces1/Es-x protein expression in different nutritional states (2 μg liver protein). Mice were fasted for 24 hours and refed for 6 hours. Fasted, refed, and fed mice were euthanized at 8:00 PM. (B) Hepatic Ces1/Es-x protein expression in different animal models of disease (*ob/ob*, leptin-deficient mice; DIO, diet-induced obesity; *Ldlr*$^{-/-}$, LDL receptor null mice fed a Western type diet) (5 μg liver protein). (C) Absence of Ces1/Es-x protein (top panels) and mRNA (bottom panels) in homozygous *Ces1/Es-x*$^{-/-}$ mice. Ces3/TGH is a related carboxylesterase migrating at a lower Mr due to lesser glycosylation and is recognized by the polyclonal anti-Ces1/Es-x antibodies. Calnexin (CNX) was used as a loading control. Bottom panels, absence of *Ces1/Es-x* mRNA expression in the liver and small intestine of *Ces1/Es-x*$^{-/-}$ mice. Cyclophilin (CYC) was used as control. (D) Body weight curves on a chow diet, with inset showing a representative photograph of wildtype and *Ces1/Es-x*$^{-/-}$ mice at 24 weeks of age (n = 6). (E) Body composition in 24-week-old mice assessed by dual x-ray absorptiometry (DEXA). Lean mass includes bone and fluids (n = 6). (F) Hematoxylin and eosin (H&E) staining of epididymal WAT (100×) and liver (200×) sections. Results represent means ± SEM. *$P < 0.05$, φ, **$P < 0.01$, $^{\#}$,***$P < 0.001$ versus wildtype.

decreased in different C57BL/6 mouse models of obesity, fatty liver, and insulin resistance including the leptin-deficient (*ob/ob*), high-fat diet-induced obese (DIO), and Western diet-induced obese *Ldlr*$^{-/-}$ mice (Fig. 1B; Supporting Fig. 1A). In mice, the expression of Ces1/Es-x protein is restricted to the liver and small intestine (Supporting Fig. 1C).

Obesity and Hepatic Steatosis in Ces1/Es-x-Deficient Mice. In order to determine the role of Ces1/Es-x in energy metabolism we generated *Ces1/Es-x*$^{-/-}$ mice (Fig. 1C; Supporting Fig. 1B,C). *Ces1/Es-x*$^{-/-}$ mice fed low-fat chow diet gained more weight than wildtype mice (Fig. 1D; Table 1). Increased body weight of *Ces1/Es-x*$^{-/-}$ mice was concomitant with an increment in white adipose tissue (WAT) weight (Fig. 1E), and larger adipocytes (Fig. 1F). Fasted *Ces1/Es-x*$^{-/-}$ mice presented with increased plasma lipid concentrations (TG, FC, CE, PL, and NEFA) (Table 1). Hepatic content of TG, FC, and CE was 300, 150, and 250% higher, respectively, relative to that of wildtype mice (Table 1). *Ces1/Es-x*$^{-/-}$ mice had a modest increase in the activity of the hepatic enzymes aspartate aminotransferase (AST) and alanine aminotransferase (ALT) in plasma, indicating mild liver damage. Histological examination of the liver showed mild steatosis in fasted *Ces1/Es-x*$^{-/-}$ mice (Fig. 1F) with no signs of acute or chronic inflammation.

Increased VLDL Secretion in Ces1/Es-x-Deficient Mice. During the postabsorptive (fasting) period plasma lipid levels primarily reflect hepatic VLDL metabolism. Fasting concentrations of plasma VLDL-TG and VLDL-cholesterol were increased in *Ces1/Es-x*$^{-/-}$ mice (Fig. 2A). VLDL secretion *in vivo* (measured following injection of P-407) was increased in *Ces1/Es-x*$^{-/-}$ mice compared to control wildtype mice (Fig. 2B). Plasma apoB levels increased in both genotypes in a similar fashion (Fig. 2C). *Ces1/Es-x*$^{-/-}$ mice presented with increased plasma apoE levels in the fasted state (Fig. 2C; Supporting Fig. 2D,E). The relative concentration of plasma apoCIII was increased and apoCII

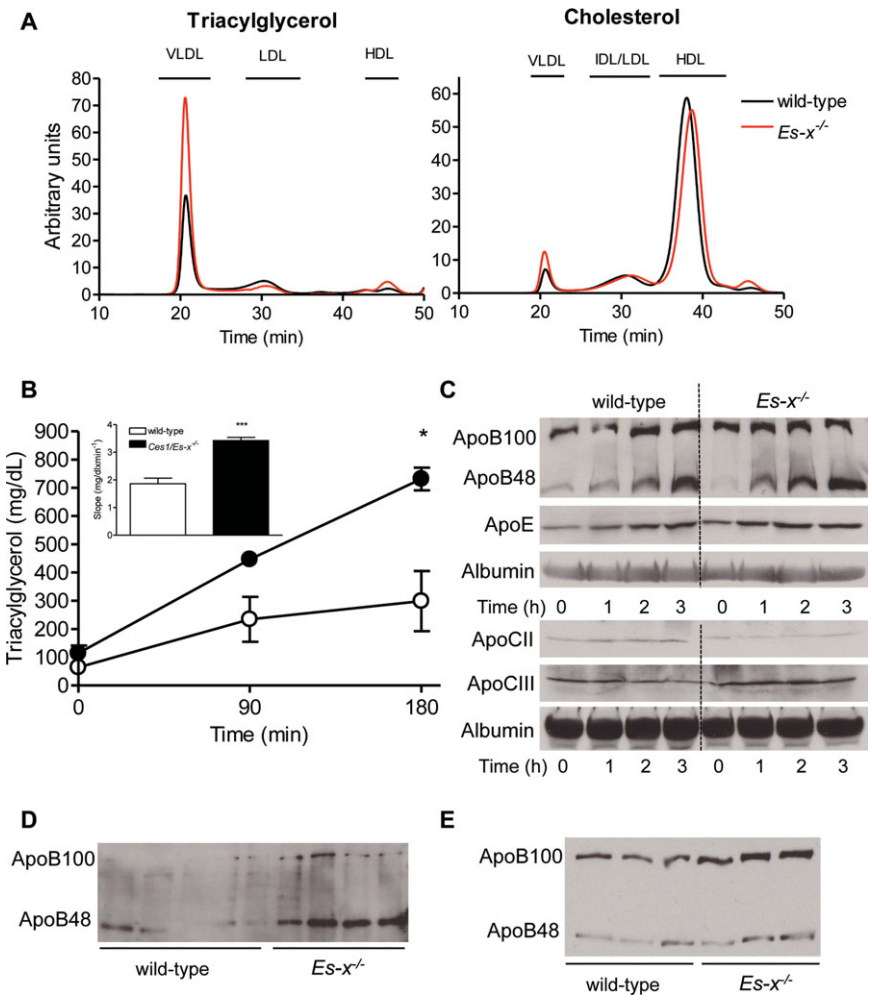

Fig. 2. Increased VLDL secretion in *Ces1/Es-x*$^{-/-}$ mice. (A) Pooled plasma from fasted mice was subjected to analyses of TG and cholesterol in lipoprotein fractions by fast-protein liquid chromatography. (B) *In vivo* VLDL secretion (n = 6). Inset shows the average slope for each curve. Statistical analysis was performed by repeated two-way ANOVA. (C) VLDL protein composition before (time 0) and after (time 1-3 h) injection of P-407. Analysis was performed by immunoblotting. (D) ApoB secretion *in vivo*. Analyses of plasma apoB concentrations was performed 2 hours after P-407 injection. (E) ApoB secretion from hepatocytes after 4-hour incubation with OA. *$P < 0.05$ versus wildtype.

concentration was decreased in *Ces1/Es-x*$^{-/-}$ mice (Fig. 2C). To differentiate newly secreted apoB from circulating apoB we injected mice intraperitoneally with [^{35}S]Met/Cys together with P-407 and followed secretion of newly synthesized radiolabeled apoB. Secretion of newly synthesized apoB100 and apoB48 was increased in *Ces1/Es-x*$^{-/-}$ mice compared to control wildtype mice (Fig. 2D) characteristic of VLDL over secretion *in vivo*. Relative lipid composition of isolated VLDL particles was similar for both genotypes (Supporting Fig. 2A). We also confirmed increased VLDL-TG (Supporting Fig. 2B), apoB100 and apoB48 secretion (Fig. 2E) from isolated *Ces1/Es-x*$^{-/-}$ hepatocytes compared to hepatocytes isolated from wildtype control mice. Interestingly, the abundance of hepatic microsomal triglyceride transfer protein (MTP) was not different between the two genotypes (Supporting Fig. 2C).

Impaired Energy Homeostasis in Ces1/Es-x-Deficient Mice. Obesity and steatosis can lead to impaired glucose metabolism. *Ces1/Es-x*$^{-/-}$ mice have lower fasting concentration of glucose (Table 1) and higher plasma insulin concentration (Table 1). The area under the curve (AUC) following an oral glucose tolerance test did not differ between genotypes (Fig. 3A), whereas *Ces1/Es-x*-deficient mice showed insensitivity to insulin (Fig. 3C). Phosphorylation of AKT, a downstream messenger in insulin signaling, was significantly increased in livers from *Ces1/Es-x*$^{-/-}$ mice when challenged with insulin (Fig. 3D). Interestingly, response to insulin (phosphorylation of AKT) in skeletal muscle and adipose tissue was significantly decreased in *Ces1/Es-x*$^{-/-}$ mice (Fig. 2E,F) relative to control.

In spite of the difference in body weight, *Ces1/Es-x*$^{-/-}$ mice consumed similar amounts of food per day as wildtype mice (Fig. 4A). Surprisingly, *Ces1/Es-x*$^{-/-}$ mice showed increased total physical activity during the dark cycle (Fig. 4B), but also presented with decreased O_2 consumption and CO_2 production (Fig. 4C,D), suggesting a net overall decrease in energy expenditure. Consistent with this, *Ces1/Es-x*$^{-/-}$ mice had an increase in the respiratory quotient (RQ) during the first period of the dark cycle (i.e., increased glucose utilization), and a decrease in the RQ during the last period of the dark cycle (i.e.,

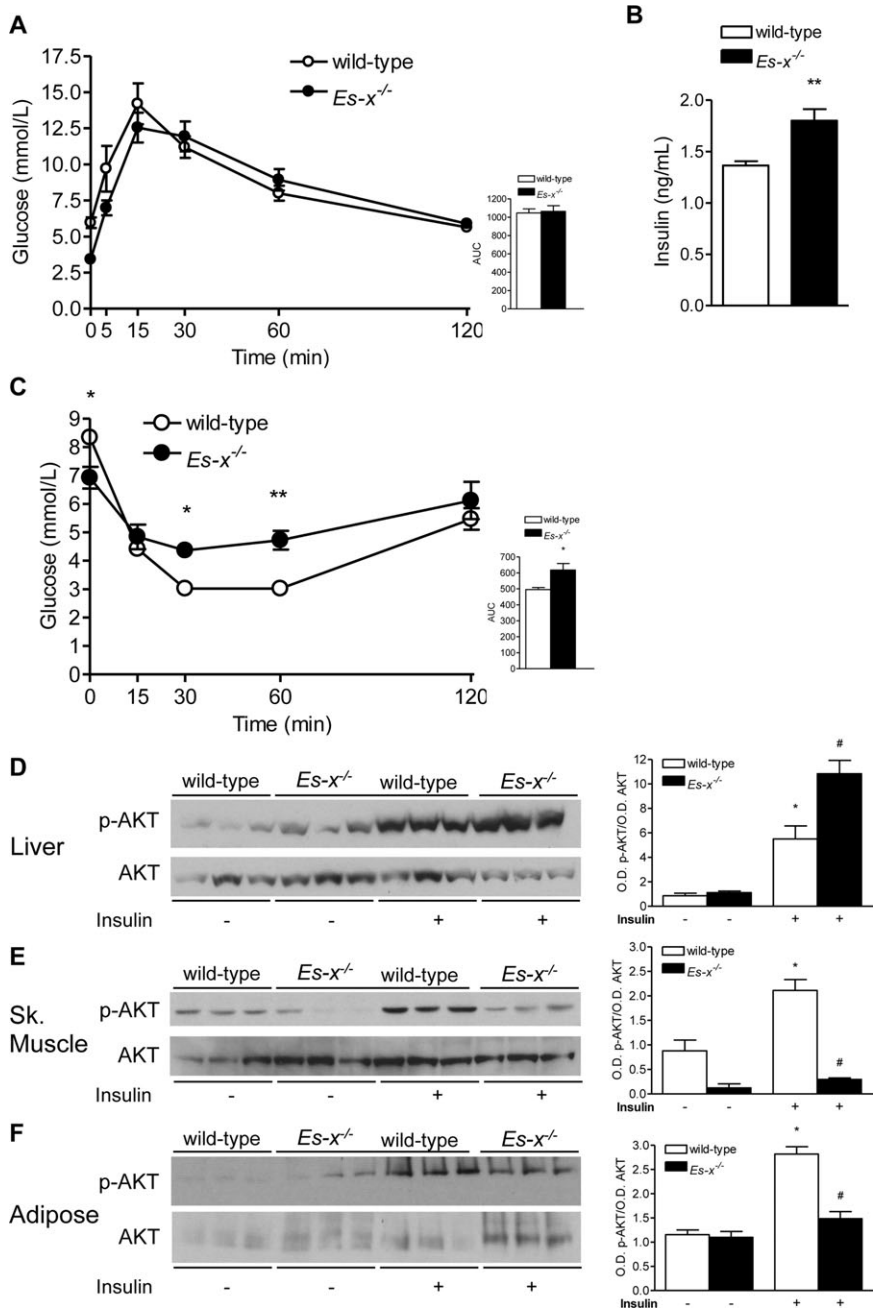

Fig. 3. Impaired insulin tolerance in the muscle and adipose but not in the liver of *Ces1/Es-x*$^{-/-}$ mice. (A) Glucose tolerance test in 24-week-old mice fasted overnight and gavaged 2 g/kg body weight (n = 6). Inset shows the mean ± SEM of the AUC. (B) Plasma insulin levels at 15 minutes of glucose tolerance test. (C) Insulin tolerance test. Mice were fasted for 6 hours and injected 1 U/kg insulin intraperitoneally (n = 6). Inset shows the mean ± SEM of the AUC. *$P < 0.05$ and **$P < 0.01$ versus wildtype. (D) Insulin sensitivity in liver. Mice were fasted for 12 hours before 0.5 U/kg body weight of bovine insulin or PBS was injected by way of the portal vein. Five minutes later the liver was removed and snap-frozen before analysis. (E,F) Insulin sensitivity in adipose tissue and skeletal muscle, respectively. Twelve-hour fasted mice were injected 1 U/kg insulin intraperitoneally. Ten minutes later adipose and skeletal muscle were removed and snap-frozen before analysis. Right panels show the ratio between O.D.s for p-AKT and AKT employed to evaluate insulin sensitivity. *$P < 0.05$ versus PBS-injected group, $^{\#}P < 0.05$ within insulin injected group.

increased utilization of FA) (Fig. 4E). Moreover, *Ces1/Es-x*$^{-/-}$ mice were found to have reduced thermogenesis relative to control (Fig. 4F; Supporting Fig. 3A), which was partly explained by (1) a trend for reduced brown adipose tissue (BAT) mass (Supporting Fig. 3B), (2) decreased expression of uncoupling protein 1 (UCP-1) after cold exposure (Supporting Fig. 3C), and (3) increased lipid storage in BAT (Supporting Fig. 3D).

Increased Hepatic Lipogenic Gene and Protein Expression in Ces1/Es-x$^{-/-}$ Mice. To further understand the mechanism of action of how *Ces1/Es-x* deficiency might contribute to hepatic steatosis, we assessed the expression of genes involved in FA synthesis and oxidation. Expression of several key genes involved in lipogenesis was found to be increased in livers from *Ces1/Es-x*$^{-/-}$ mice relative to control, particularly the master lipogenic transcription factor SREBP-1c, fatty acid synthase (FAS), stearoyl-CoA desaturase 1 (SCD-1), acyl-CoA:monoacylglycerol acyltransferase 2 (MGAT2), and SREBP-2, a transcription factor regulating the expression of cholesterol synthesis (Fig. 5A). No significant differences were observed between genotypes in the hepatic expression of mRNA encoding MGAT1, acyl-CoA:diacylglycerol acyltransferase 1 and 2 (DGAT-1 and -2), FA oxidation enzymes/transporters (with the exception of augmented *Ucp2* expression and decreased

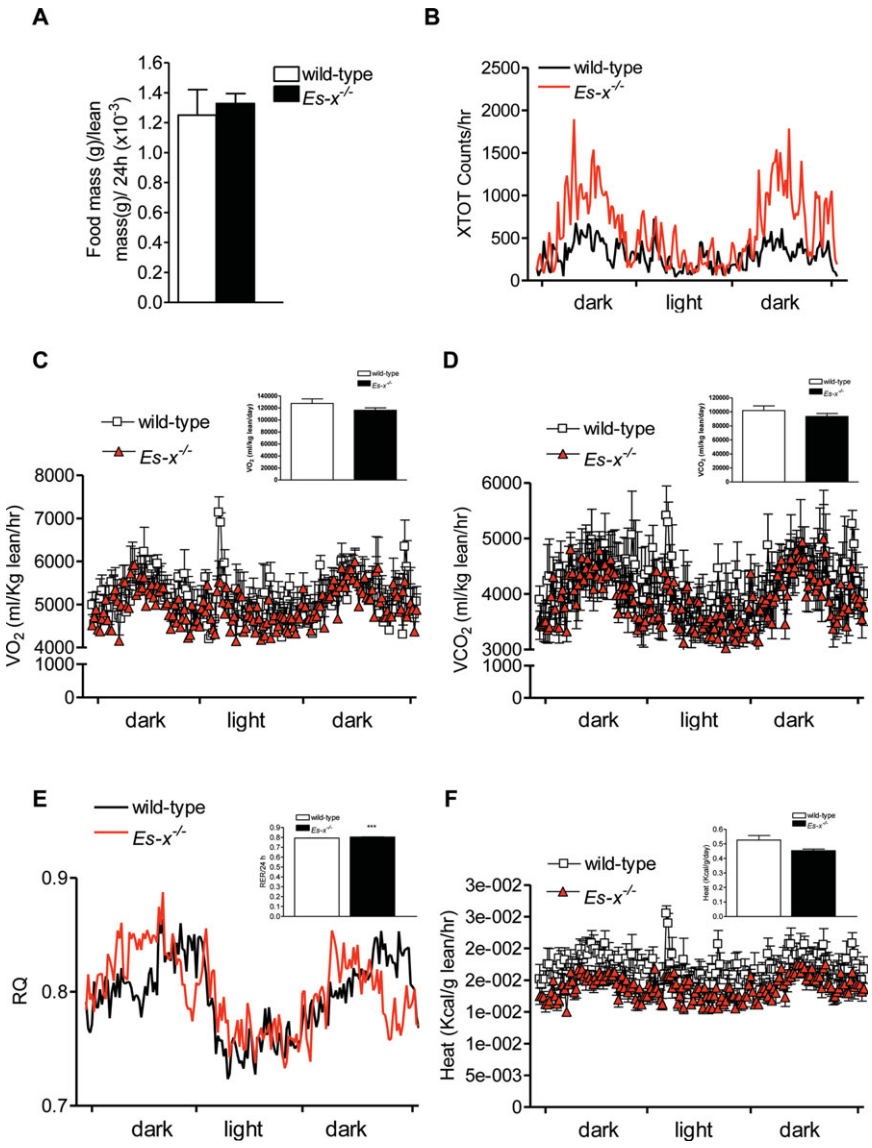

Fig. 4. *Ces1/Es-x*$^{-/-}$ mice show impaired energy metabolism. (A) Food intake per day. (B) Total locomotor activity with inset showing the mean ± SEM during the light and dark periods over a 24-hour period. (C) Oxygen consumption curves. Inset shows the mean ± SEM over a 24-hour period. (D) Carbon dioxide production curves. Inset shows the mean ± SEM over a 24-hour period. (E) Respiratory quotient (RQ) curve with inset showing the mean ± SEM over a 24-hour period. (F) Heat production curves, with inset showing the mean ± SEM over a 24-hour period. (For all experiments n = 6.) ***$P < 0.001$ versus wildtype.

Lcad expression), and lipases (Fig. 5A). To further confirm the activation of SREBP-1c, the abundance of nuclear SREBP-1c was analyzed by immunoblotting. The amount of active SREBP-1c in the nucleus was found to be higher (fasted state) in *Ces1/Es-x*$^{-/-}$ mice compared to wildtype (Fig. 5B).

Increased Lipogenesis in Ces1/Es-x*$^{-/-}$ *Hepatocytes. To appreciate the contribution by which *Ces1/Es-x* deficiency leads to increased lipogenesis and steatosis, mouse primary hepatocytes were isolated and metabolic lipid labeling studies were performed. The increased SREBP-1c processing and expression of lipogenic genes resulted in significant up-regulation of *de novo* lipogenesis in *Ces1/Es-x*-deficient mice (Fig. 5C). Incubation of hepatocytes from *Ces1/Es-x*$^{-/-}$ mice with OA resulted in an increased number of lipid droplets compared to control wildtype hepatocytes (Supporting Fig. 4A). However, the incorporation of exogenously supplied radiolabeled OA into different lipid species was similar in hepatocytes from both genotypes, although lipid mass was significantly higher at all times in hepatocytes from *Ces1/Es-x*$^{-/-}$ mice (Supporting Fig. 4B).

Hepatocytes from Ces1/Es-x*$^{-/-}$ *Mice Accumulate TG Enriched in PUFA. Because *Ces1/Es-x* deficiency results in increased nuclear SREBP levels and because SREBP processing has been shown to be attenuated by PUFA,[13-15] we hypothesized that Ces1/Es-x might catalyze the release of PUFA from cellular lipids. Incubation of *Ces1/Es-x*$^{-/-}$ hepatocytes with EPA and DHA reversed the increased lipogenic phenotype (Fig. 5D). The antilipogenic effect was mediated by lower nuclear SREBP-1c upon PUFA treatment (Fig. 5E). Hepatocytes from chow diet-fed *Ces1/Es-x*$^{-/-}$ mice accumulated significantly more EPA and DHA in TG in addition to palmitoleic acid compared to control hepatocytes,

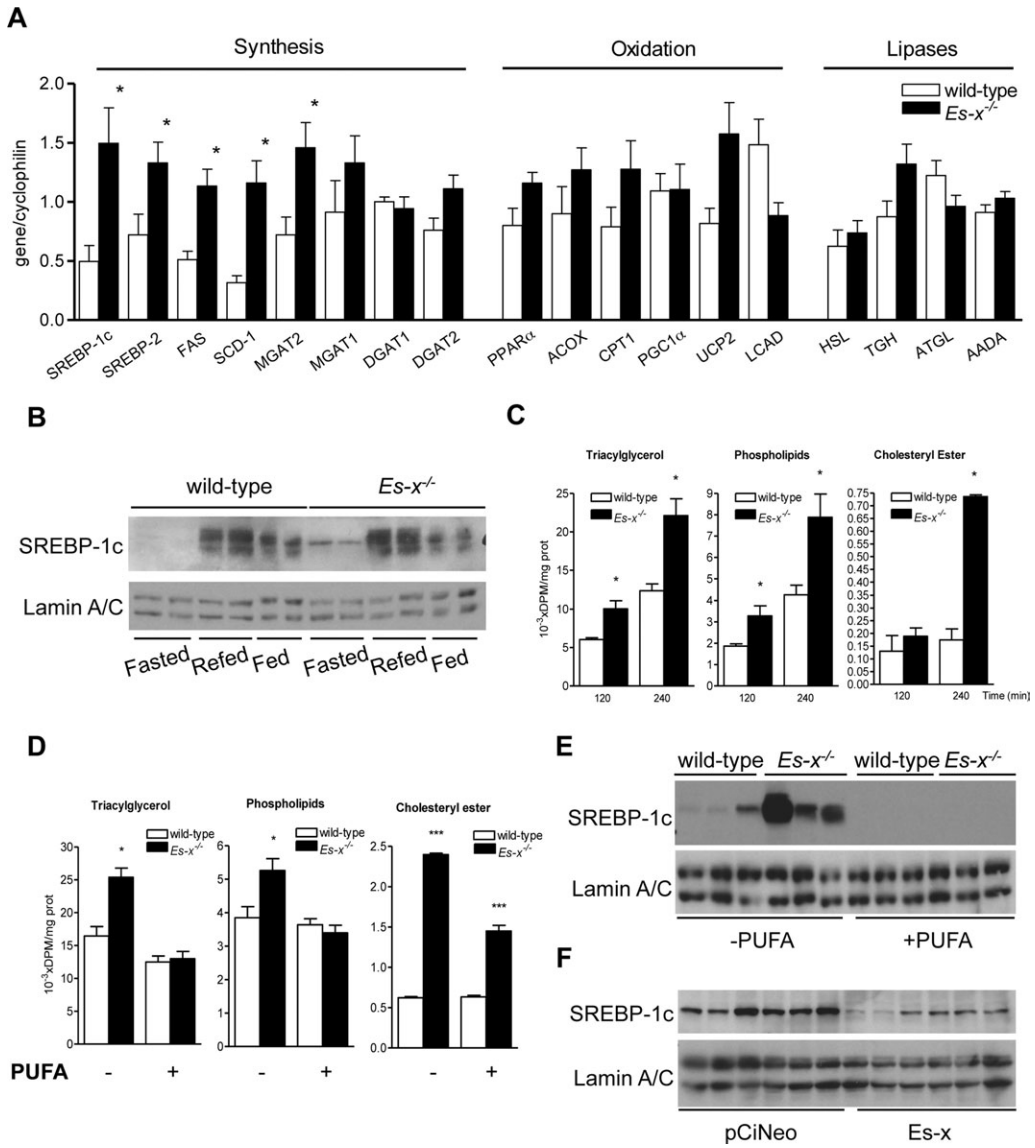

Fig. 5. Hepatocytes from *Ces1/Es-x*$^{-/-}$ mice show increased lipogenesis. (A) Hepatic expression of lipogenic, oxidation and lipase genes in livers from 24-week-old mice by qPCR. (B) Hepatic nuclear levels of SREBP-1c. Image shows an immunoblot representative of three independent experiments. (C) *De novo* lipogenesis: Incorporation of radiolabeled acetic acid into lipids. (D) Radiolabeled acetate incorporation by hepatocytes incubated with or without PUFA. Bars represent mean ± SEM. *$P < 0.05$, ***$P < 0.001$. (E) Nuclear levels of SREBP-1c in cultured hepatocytes. Image shows an immunoblot representative of three independent experiments. (F) Nuclear levels of SREBP-1c in McArdle RH-7777 cells expressing an empty vector (pCiNeo) or Ces1/Es-x cDNA incubated in a low-glucose, serum-free medium for 4 hours. Three independent experiments were performed for *in vitro* studies.

whereas the concentration of saturated stearic acid in TG was decreased (Supporting Fig. 5A,B). No FA species differences were observed in any other lipid classes between genotypes (not shown). Conversely, ectopic expression of *Ces1/Es-x* in rat hepatoma cells resulted in decreased amounts of PUFA incorporated in TG (Supporting Fig. 5C) and decreased nuclear SREBP-1c levels (Fig. 5F). No change in the relative FA content in any other lipid class was observed (not shown). To assess the specificity of Ces1/Es-x for PUFA in TG, we tested Ces1/Es-x-regulated release of PUFA from endogenously synthesized [^{14}C]EPA- and DHA-, as well as [^{3}H]oleate-labeled lipids in the ER. Ces1/Es-x-expressing cells had decreased oleate- and PUFA-labeled TG (Supporting Fig. 5D,F, time 0) compared to control cells. No other differences in the incorporation of FA into other lipid classes (PL, CE) were observed (data not shown). Despite the lower microsomal PUFA-labeled TG levels in Ces1/Es-x-containing microsomes, the concentration of free [^{14}C]EPA and DHA were similar between control and Ces1/Es-x-containing microsomes, suggesting increased release of PUFA by Ces1/Es-x (Supporting Fig. 5E, time 0). The rate of PUFA release from preformed lipids (Supporting Fig. 4E) but not of oleate

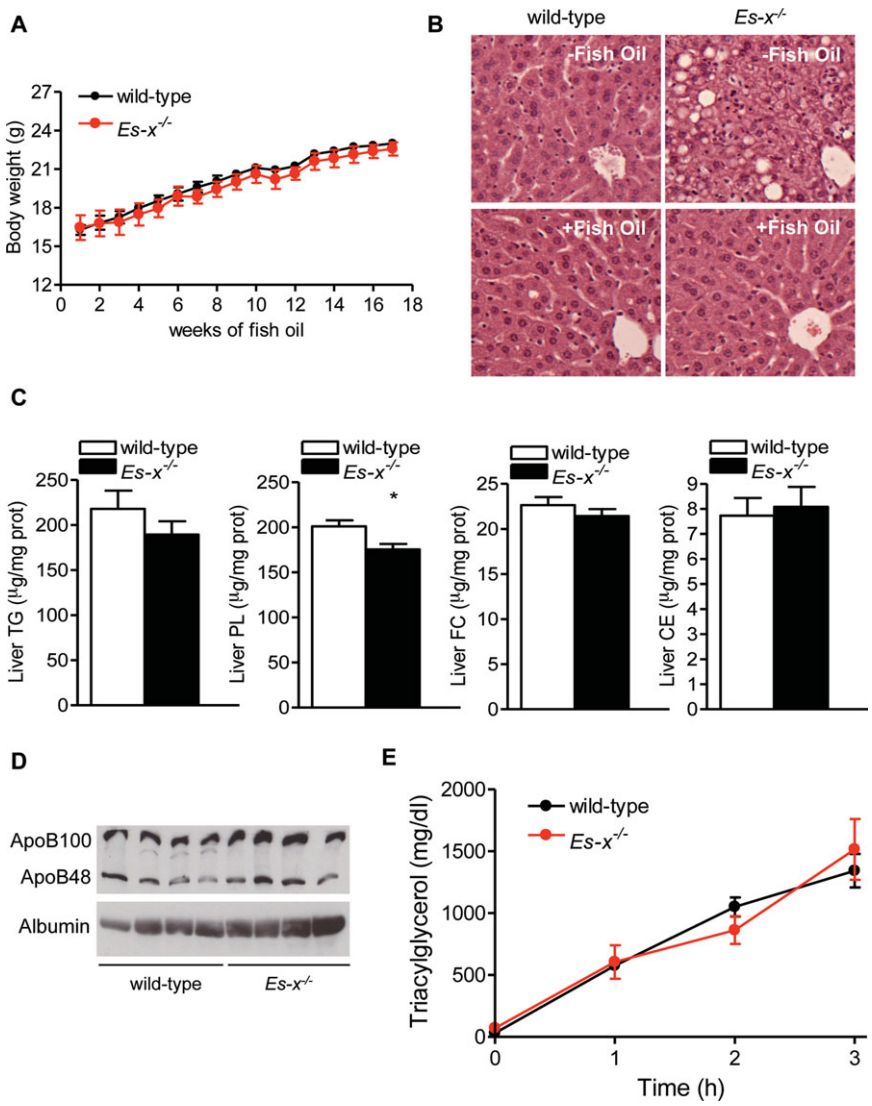

Fig. 6. Fish oil supplementation reverses the obese phenotype of Ces1/Es-x deficiency. (A) Body weight curves. Animals were on a chow diet and supplemented with 200 μL fish oil daily for 4 months (n = 5). (B) H&E staining of liver sections (200×) from mice supplemented with or without fish oil. (C) Liver lipid levels after fish oil supplementation. Bars represent mean ± SEM. *$P < 0.05$. (D) Plasma apoB100 and apoB48 levels after 4 months of fish oil supplementation. (E) *In vivo* VLDL secretion from mice supplemented with fish oil for 4 months.

(Supporting Fig. 5G) was increased in Ces1/Es-x-containing microsomes, indicating the preference of Ces1/Es-x for PUFA-enriched TG over oleate-enriched TG.

Dietary Fish Oil Supplementation Completely Reverses the Obese Phenotype of* Ces1/Es-x *Deficiency. To assess whether PUFA supplementation could reverse the lipogenic phenotype in *Ces1/Es-x*$^{-/-}$ mice *in vivo*, animals were fed a diet supplemented with fish oil for 4 months. Fish oil supplementation completely prevented weight gain in *Ces1/Es-x*$^{-/-}$ mice when compared to mice fed standard chow (Fig. 6A versus Fig. 1B), resulting in comparable body weights of *Ces1/Es-x*$^{-/-}$ and control wildtype mice at the end of the dietary intervention (Table 2). Although fish oil supplementation had no effect on blood glucose disposal in *Ces1/Es-x*$^{-/-}$ mice (Table 2 versus Table 1), plasma TG, PL, and FC concentrations were comparable to wildtype mice (Table 2). Fish oil supplementation completely abolished the steatosis observed in livers from fasted *Ces1/Es-x*$^{-/-}$ mice fed standard chow (Fig. 6B). Accordingly, upon fish oil supplementation, hepatic lipid mass was comparable between the two genotypes (Fig. 6C). ApoB100, -B48, and VLDL-TG secretions were also normalized in *Ces1/Es-x*$^{-/-}$ mice upon fish oil supplementation (Fig. 6D,E). No differences in the activity of the hepatic enzymes AST and ALT in plasma were observed between genotypes upon fish oil supplementation (Table 2).

Analysis of hepatic FA composition showed increased accumulation of DHA in TG in *Ces1/Es-x*$^{-/-}$ mice supplemented with fish oil (Supporting Fig. 6). No differences between the genotypes were observed in any other any other fatty acids or in other lipid species (not shown).

Table 2. Body Weight and Plasma Biochemical Parameters Upon Fish Oil Supplementation

	Wildtype	*Ces1/Es-x*$^{-/-}$
Body weight (g)	23.12 ± 0.40	21.62 ± 0.44*
Plasma TG (mg/dL)	21.58 ± 5.54	15.41 ± 4.41
Plasma FC (mg/dL)	13.64 ± 0.45	12.26 ± 0.33
Plasma CE (mg/dL)	16.17 ± 2.09	10.39 ± 0.84
Plasma PL (mg/dL)	65.66 ± 7.01	54.26 ± 3.39
NEFA (mEq/L)	1.311 ± 0.151	1.249 ± 0.111
AST (U/L)	93.46 ± 5.84	84.59 ± 5.63
ALT (U/L)	40.74 ± 2.76	42.24 ± 5.31
Glucose (mmol/L)	4.23 ± 0.13	3.33 ± 0.09**

n=5.
*$P < 0.05$.
**$P < 0.005$.

Discussion

The results from this study show that Ces1/Es-x plays an important role in regulating lipid synthesis, secretion, and energy metabolism. *Ces1/Es-x*$^{-/-}$ mice present with increased lipogenesis accompanied with insulin resistance, hyperinsulinemia, and decreased energy expenditure. Consequently, *Ces1/Es-x*$^{-/-}$ mice become obese even on a standard chow diet and develop hepatic steatosis and hyperlipidemia.

Ces1/Es-x protein expression appears to be responsive to nutritional regulation. It was previously reported that diet supplementation with bile salt cholate or with bile acid-binding resin cholestyramine induced hepatic expression of *Ces1/Es-x* mRNA.[8] Ces1/Es-x protein is expressed only in the liver and the small intestine, and its hepatic expression decreases during fasting, a condition when hepatic lipid storage is induced and VLDL secretion is high.

Plasma of Ces1/Es-x-deficient mice have increased fasting apoE levels (which inhibits LPL activity, thereby increasing plasma TG levels,[16,17] although opposite effects have also been postulated[18]), findings in line with positive correlation between hepatic apoE expression and VLDL production. Importantly, we observed an increment in apoCIII (inhibitor of LpL) and a decrease in apoCII (activator of LpL) protein levels in *Ces1/Es-x*$^{-/-}$ mice, which may influence clearance of TG-rich lipoproteins. These factors, together with increased apoB secretion, contribute to the hyperlipidemia observed in *Ces1/Es-x*$^{-/-}$ mice, which in turn might influence the lipid deposition in peripheral tissues and accretion of body weight.

Excessive lipid supply to skeletal muscle, liver, and pancreas is believed to be one of the main causes of insulin resistance[19] and is the likely contributor to impaired insulin tolerance in *Ces1/Es-x*-deficient mice. Insulin signaling is severely compromised in adipose and skeletal muscle tissues in *Ces1/Es-x*$^{-/-}$ mice, whereas in the liver insulin signaling is enhanced. As demonstrated in other models,[20] the liver of *Ces1/Es-x*$^{-/-}$ mice seems to compensate for the loss of insulin sensitivity and glucose utilization in peripheral tissues in spite of the lipid excess. *Ces1/Es-x*$^{-/-}$ mice presented with reduced fasting glycemia. In line with this observation, and because of normal insulin signaling in the liver observed in *Ces1/Es-x*$^{-/-}$ mice, there were no differences between genotypes in hepatic expression of gluconeogenic genes or in pyruvate tolerance tests (data not shown).

The weight gain in *Ces1/Es-x*$^{-/-}$ mice is not due to increased food consumption, but rather to impaired energy utilization. Indeed, *Ces1/Es-x*$^{-/-}$ mice present with a very interesting RQ curve: during the first half of the dark period, *Ces1/Es-x*$^{-/-}$-deficient mice show a high carbohydrate to fat utilization ratio, which indicates increased oxidation of carbohydrates. However, in the second half of the dark period, *Ces1/Es-x*$^{-/-}$ mice appear to suddenly shift whole-body substrate metabolism from mostly carbohydrate to one that is derived predominately from fat oxidation. Overall, *Ces1/Es-x*$^{-/-}$ mice seem to favor carbohydrate over fat utilization, which leads to decreased plasma glucose levels, increased lipid storage, and the obese phenotype. These results are similar to those from BAT-less mice; these animals developed cold intolerance, obesity, and insulin resistance[21,22] due to incapacity to dissipate excess energy by the so-called diet-induced thermogenesis.

The increased hepatic lipogenesis in *Ces1/Es-x*$^{-/-}$ mice is due to the activation of the master transcription factors controlling lipogenesis and sterol biosynthesis SREBP-1c and -2, respectively. In the liver, SREBP-1c processing is activated by insulin, by liver X receptor (LXR) α (which in turn is activated by oxysterols), and is suppressed by PUFA. Hyperinsulinemia observed in *Ces1/Es-x*$^{-/-}$ mice could be partially responsible for increased SREBP-1c expression. However, when primary hepatocytes (wildtypes and *Ces1/Es-x*$^{-/-}$) or McArdle cells (expressing Ces1/Es-x DNA) are cultured in serum-free media (no insulin), the corresponding phenotypes still persist. Hepatic LXRα mRNA expression, as well as the expression of corresponding LXRα target genes, remained unchanged in *Ces1/Es-x*$^{-/-}$ mice (data not shown). It is known that PUFA suppress the activity of SREBP-1c promoter independently of LXR[13]; furthermore, PUFA enhance the degradation of *Srebp-1c* mRNA[15] and stimulate proteasomal degradation of SREBP proteins.[14] We hypothesized that PUFA released from TG

stores by Ces1/Es-x might play a key role in the inactivation of SREBP-1c processing (Supporting Fig. 7). This mechanism is supported by the accumulation of EPA and DHA in hepatic TG in *Ces1/Esx*$^{-/-}$ mice and increased lipogenesis; and conversely ectopic expression of *Ces1/Es-x* resulted in increased PUFA release from microsomal TG, decreased nuclear SREBP-1c, and decreased lipogenesis. Nutritional supplementation with fish oil completely reversed the obese phenotype of *Ces1/Es-x*$^{-/-}$ mice, leading to a comparable weight gain as control wildtype mice and reduced blood and hepatic lipid concentrations. An interesting finding is that TG from *Ces1/Es-x*$^{-/-}$ mice livers accumulated exclusively DHA. These results not only support the hypothesis that Ces1/Es-x is playing a role in selective hydrolysis of PUFA from TG, but also indicate that PUFA supplied from fish oil are responsible for the reversal of the lipogenic phenotype in *Ces1/Es-x*$^{-/-}$ mice.

In summary, our studies have identified Ces1/Es-x as a novel regulator of lipogenesis and apoB-containing lipoprotein secretion in the liver. This regulatory mechanism involves catalytic function of Ces1/Es-x that releases PUFA from intracellular TG leading to inhibition of SREBP-1c mediated lipogenesis.

Acknowledgment: We thank Edward A. Armstrong for expert technical assistance, Dr. Jelske van der Veen for discussions and article editing, and Drs. Michael Brown and Joseph Goldstein (University of Texas Southwestern Medical Center) for anti-SREBP-1c polyclonal antibodies. Some lipid analyses were performed by the Lipid Analysis Core, which receives support from the Women and Children Health Research Institute.

References

1. van den Berghe G. The role of the liver in metabolic homeostasis: implications for inborn errors of metabolism. J Inherit Metab Dis 1991;14:407-420.
2. Samuel VT, Liu ZX, Qu X, Elder BD, Bilz S, Befroy D, et al. Mechanism of hepatic insulin resistance in non-alcoholic fatty liver disease. J Biol Chem 2004;279:32345-32353.
3. Sanyal AJ. Mechanisms of Disease: pathogenesis of nonalcoholic fatty liver disease. Nat Clin Pract Gastroenterol Hepatol 2005;2:46-53.
4. Holmes RS, Wright MW, Laulederkind SJ, Cox LA, Hosokawa M, Imai T, et al. Recommended nomenclature for five mammalian carboxylesterase gene families: human, mouse, and rat genes and proteins. Mamm Genome 2010;21:427-441.
5. Gilham D, Ho S, Rasouli M, Martres P, Vance DE, Lehner R. Inhibitors of hepatic microsomal triacylglycerol hydrolase decrease very low density lipoprotein secretion. Faseb J 2003;17:1685-1687.
6. Wei E, Ben Ali Y, Lyon J, Wang H, Nelson R, Dolinsky VW, et al. Loss of TGH/Ces3 in mice decreases blood lipids, improves glucose tolerance, and increases energy expenditure. Cell Metab 2010;11:183-193.
7. Dolinsky VW, Gilham D, Alam M, Vance DE, Lehner R. Triacylglycerol hydrolase: role in intracellular lipid metabolism. Cell Mol Life Sci 2004;61:1633-1651.
8. Ellinghaus P, Seedorf U, Assmann G. Cloning and sequencing of a novel murine liver carboxylesterase cDNA. Biochim Biophys Acta 1998;1397:175-179.
9. Kennedy AR, Pissios P, Otu H, Roberson R, Xue B, Asakura K, et al. A high-fat, ketogenic diet induces a unique metabolic state in mice. Am J Physiol Endocrinol Metab 2007;292:E1724-1739.
10. Flowers MT, Keller MP, Choi Y, Lan H, Kendziorski C, Ntambi JM, et al. Liver gene expression analysis reveals endoplasmic reticulum stress and metabolic dysfunction in SCD1-deficient mice fed a very low-fat diet. Physiol Genomics 2008;33:361-372.
11. Ko KW, Erickson B, Lehner R. Es-x/Ces1 prevents triacylglycerol accumulation in McArdle-RH7777 hepatocytes. Biochim Biophys Acta 2009;1791:1133-1143.
12. Azzout-Marniche D, Becard D, Guichard C, Foretz M, Ferre P, Foufelle F. Insulin effects on sterol regulatory-element-binding protein-1c (SREBP-1c) transcriptional activity in rat hepatocytes. Biochem J 2000;350(Pt 2):389-393.
13. Deng X, Cagen LM, Wilcox HG, Park EA, Raghow R, Elam MB. Regulation of the rat SREBP-1c promoter in primary rat hepatocytes. Biochem Biophys Res Commun 2002;290:256-262.
14. Jump DB, Botolin D, Wang Y, Xu J, Christian B, Demeure O. Fatty acid regulation of hepatic gene transcription. J Nutr 2005;135:2503-2506.
15. Xu J, Teran-Garcia M, Park JH, Nakamura MT, Clarke SD. Polyunsaturated fatty acids suppress hepatic sterol regulatory element-binding protein-1 expression by accelerating transcript decay. J Biol Chem 2001;276:9800-9807.
16. Fojo SS, Brewer HB. Hypertriglyceridaemia due to genetic defects in lipoprotein lipase and apolipoprotein C-II. J Intern Med 1992;231:669-677.
17. Rensen PC, van Berkel TJ. Apolipoprotein E effectively inhibits lipoprotein lipase-mediated lipolysis of chylomicron-like triglyceride-rich lipid emulsions in vitro and in vivo. J Biol Chem 1996;271:14791-14799.
18. Huang Y, Liu XQ, Rall SC Jr, Taylor JM, von Eckardstein A, Assmann G, et al. Overexpression and accumulation of apolipoprotein E as a cause of hypertriglyceridemia. J Biol Chem 1998;273:26388-26393.
19. Bergman RN, Ader M. Free fatty acids and pathogenesis of type 2 diabetes mellitus. Trends Endocrinol Metab 2000;11:351-356.
20. Cho Y, Ariga M, Uchijima Y, Kimura K, Rho JY, Furuhata Y, et al. The novel roles of liver for compensation of insulin resistance in human growth hormone transgenic rats. Endocrinology 2006;147:5374-5384.
21. Hamann A, Flier JS, Lowell BB. Decreased brown fat markedly enhances susceptibility to diet-induced obesity, diabetes, and hyperlipidemia. Endocrinology 1996;137:21-29.
22. Lowell BB, V SS, Hamann A, Lawitts JA, Himms-Hagen J, Boyer BB, et al. Development of obesity in transgenic mice after genetic ablation of brown adipose tissue. Nature 1993;366:740-742.